

Supplementary Information

A Hybrid Organic-Inorganic Three- Dimensional Cathode Interfacial Material for Organic Solar Cells

Menglan Lv^{a,b,c*}, Jacek J. Jasieniak^d, Jin Zhu^c, Xiwen Chen^{b*}

^a Guizhou Institute of Technology, Guiyang, 550003, China.

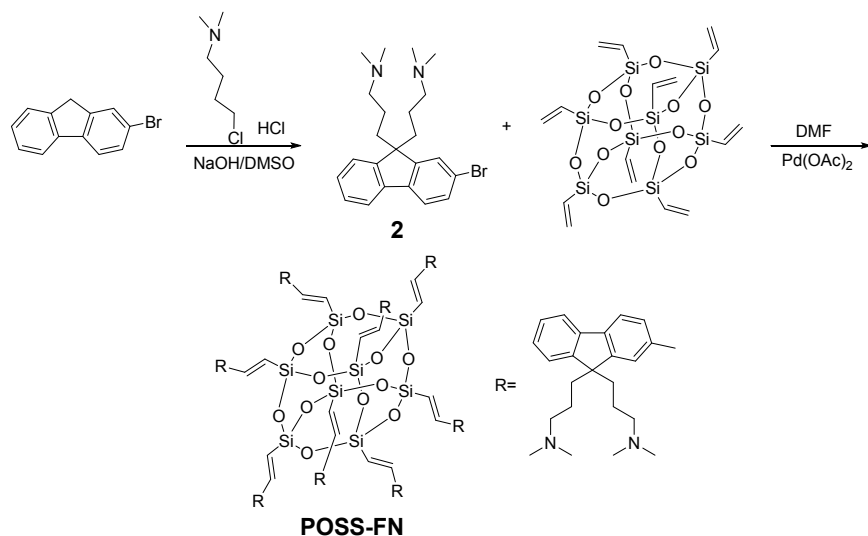
^b CSIRO Manufacturing flagship, Clayton, VIC 3168, Australia.

^c Chengdu Institute of Organic Chemistry, Chinese Academy of Sciences,
Chengdu, 610041, China.

^d Department of Materials Science and Engineering, Monash University, Clayton,
VIC 3800, Australia.

1. Materials

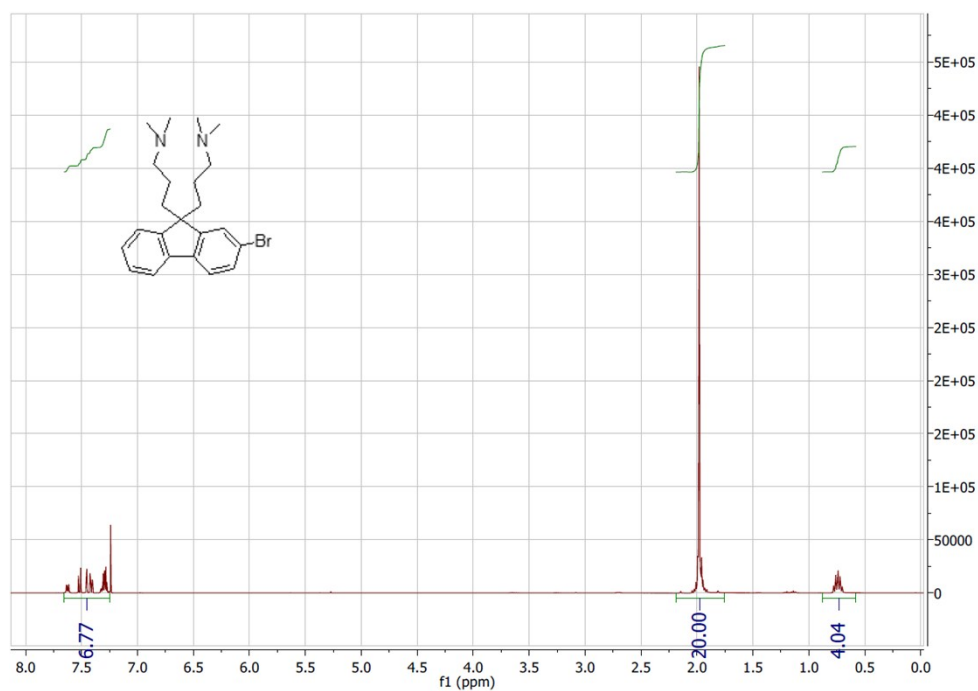
The synthesis of POSS-FN is illustrated in **Scheme S1** as below:



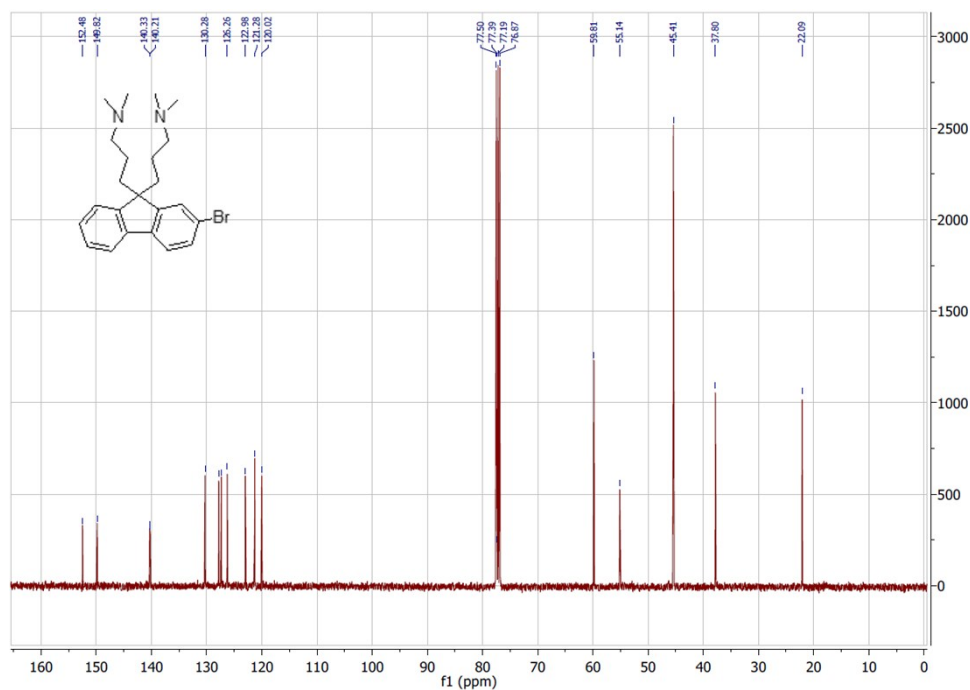
Scheme S1 Synthesis route of POSS-FN.

Synthesis of (9,9-bis(3'-(N,N-dimethylamino)propyl)-2-bromofluorene (compound 2) [S1]

2-bromofluorene (3.0 g, 12 mmol), tetrabutylammonium bromide (80 mg) and DMSO (50 mL) were placed in a 250 mL two-neck flask under nitrogen atmosphere. Then, 12 mL of a 50 wt % aqueous solution of sodium hydroxide was injected, and 20 mL of 3-dimethylaminopropylchloride hydrochloride (5.0 g, 32 mmol) solution in DMSO was added slowly to the mixture. The reaction mixture was stirred at 45 °C overnight at which time the reaction was judged completed by TLC (ethyl acetate and triethylamine as the eluent). The mixture was diluted with 50 mL of water, to dissolve all salts. The product was extracted with ether three times and the combined organic layers were washed with water, and brine respectively. The solution was dried over MgSO₄ and stripped off the solvent by vacuum evaporation to yield a crude orange grease. This crude grease was purified by column chromatography by eluting first with dichloromethane and methanol in a 50:1 ratio with 10% triethylamine and then in a 100:1 ratio including 10% triethylamine. The product compound **2** was isolated as a colorless crystals (3.0 g, 60%).¹H NMR (400 MHz, CDCl₃, δ): 7.60-7.65 (m, 1H; Ar-H), 7.50-7.53(m, 1H; Ar-H), 7.40-7.46(m, 2H; Ar-H), 7.29-7.33(m, 3H; Ar-H), 1.81-1.98 (m, 20H; Ar-C-CH₂-, -N-CH₂-, -N-CH₃), 0.70-0.78 (m, 4H; -CH₂-); ¹³C NMR (100 MHz, CDCl₃, δ): 152.5, 149.8, 140.3, 140.2, 130.3, 126.3, 123.0, 121.3, 120.0, 59.8, 55.1, 45.4, 37.8, 22.1.



(a)

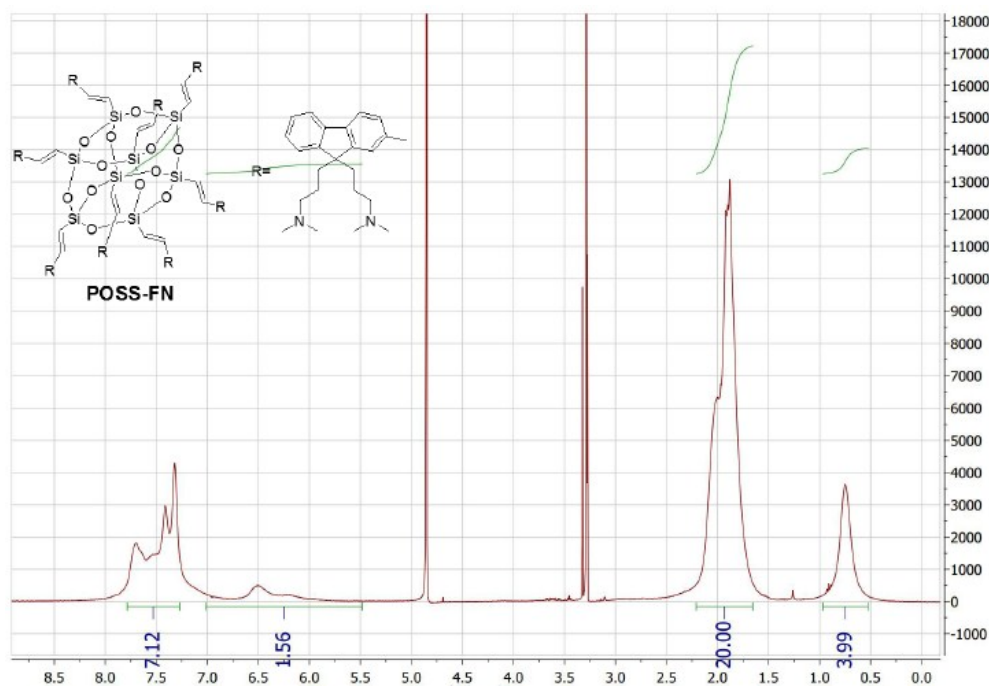


(b)

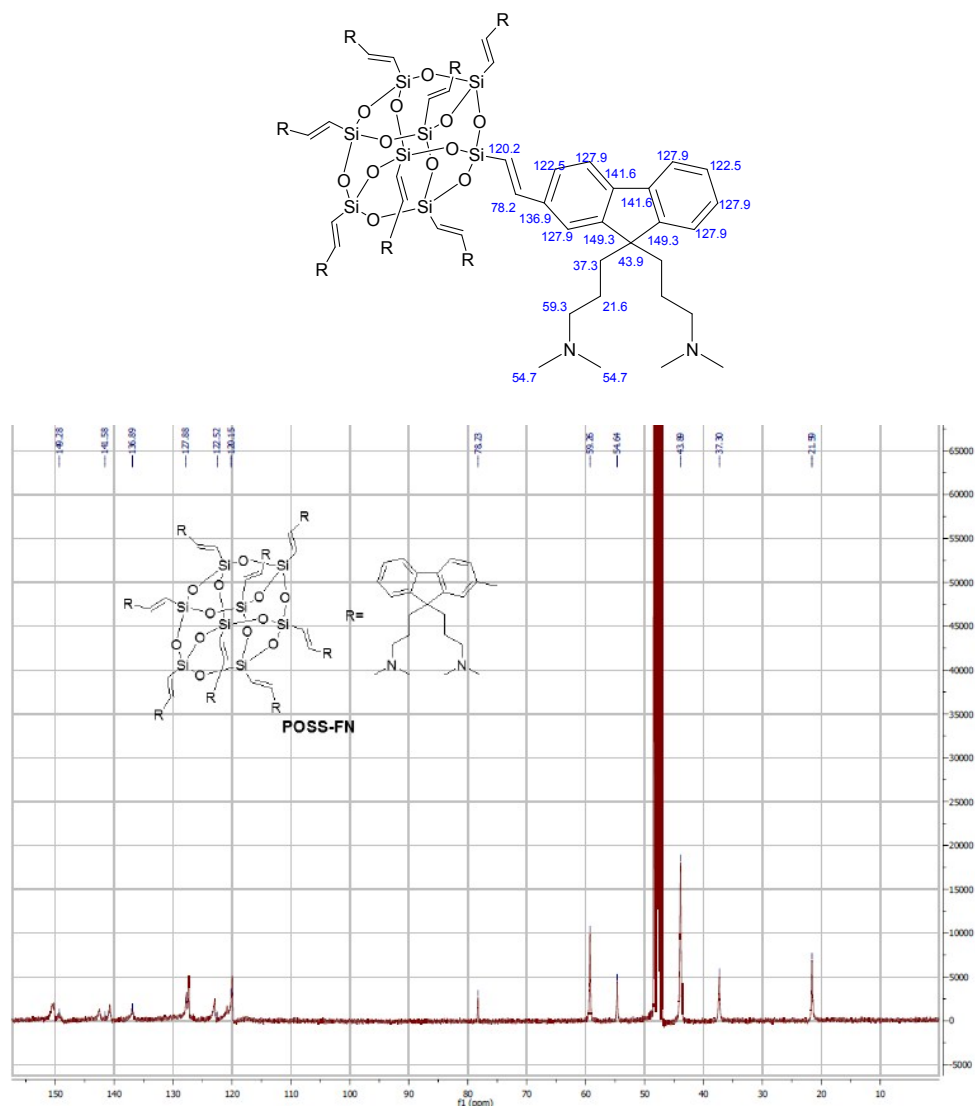
Figure S1. (a) ¹H NMR; (b) ¹³C NMR in CDCl₃ spectra of compound 2.

Synthesis of 1,3,5,7,9,11,13,15-(9-bis(3'-(N,N-dimethylamino)propyl)-2,7-fluorene))-octavinylpentacyclo-octasiloxane (POSS-FN) [S2]

POSS (48 mg, 0.076 mmol), compound **2** (315 mg, 0.76 mmol) and tri-*o*-tolylphosphine (100 mg, 0.33 mmol) were placed in a microwave reaction tube (5 mL). A mixture of DMF (2.0 mL) and triethylamine (1.0 mL) was added to the tube, and the reaction vessel was degassed for 15 min. Pd(OAc)₂ (13.7 mg, 0.60 mmol) was added to the mixture, and then the reaction mixture was degassed again. The mixture was stirred at 140 °C for 2h in a microwave reactor. Then the mixture was filtered and the precipitate was collected and washed with acetone. The crude solid was purified by recycle GPC, and the product was isolated as a colorless crystal POSS-FN (100 mg, 39.8%). ¹H NMR (400 MHz, MeOD, δ): 7.01-7.95 (m, 7H; Ar-H), 5.75-6.89 (m, 2H; -CH=CH-), 1.49-2.28 (m, 20H; Ar-C-CH₂-, -N-CH₂-, -N-CH₃), 0.53-0.99 (m, 4H; -CH₂-). ¹H NMR (400 MHz, CDCl₃, δ): 7.32-7.85 (m, 7H; Ar-H), 5.70-6.73 (m, 2H; -CH=CH-), 1.58-2.24 (m, 20H; Ar-C-CH₂-, -N-CH₂-, -N-CH₃), 0.54-0.93 (m, 4H; -CH₂-). ¹³C NMR (100 MHz, CDCl₃, δ): 149.3, 141.6, 136.9, 127.9, 122.5, 120.2, 78.2, 59.3, 54.7, 43.9, 37.3, 21.6.



(a)



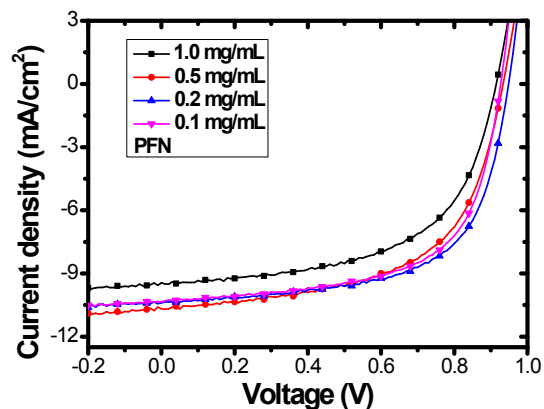


Figure S3. J-V curves of devices with PFN interlayer spin casted from methanol solutions.

Table S2. The device performance with POSS-FN cathode interlayer.

POSS-FN Concentration [mg/mL]	Voc [V]	Jsc [mA/cm ²]	FF [%]	PCE [%]	Rs [Ωcm^2]	Rsh [k Ωcm^2]
0.05	0.93	9.88	63.1	5.80	8.22	50.7
0.1	0.95	10.2	62.9	6.10	4.23	82.3
0.2	0.94	10.4	63.0	6.17	1.76	94.1
0.5	0.91	10.2	58.1	5.41	9.95	26.9
1.0	0.88	9.27	49.9	4.07	29.1	10.7

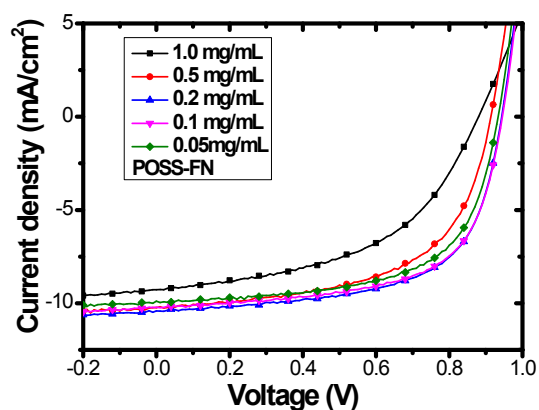


Figure S4. J-V curves of devices with POSS-FN interlayer spin casted from methanol solutions.

Table S3. The device performance with PStN cathode interlayer.

PStN Concentration [mg/mL]	Voc [V]	Jsc [mA/cm ²]	FF [%]	PCE [%]	Rs [Ωcm^2]	Rsh [$\text{k}\Omega\text{cm}^2$]
0.05	0.95	10.4	61.7	6.10	1.34	96.6
0.1	0.96	10.2	59.0	5.80	9.85	55.4
0.2	0.94	9.04	61.3	5.21	12.5	27.8
0.5	0.94	9.59	45.4	4.09	60.6	19.8
1.0	0.90	7.76	24.1	1.68	979	1.22

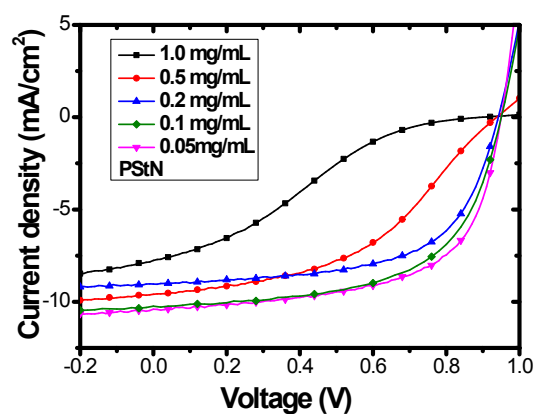


Figure S5. J-V curves of devices with PStN interlayer spin casted from methanol solutions.

3. The roughness analysis of conducting atomic microscopy (AFM) images

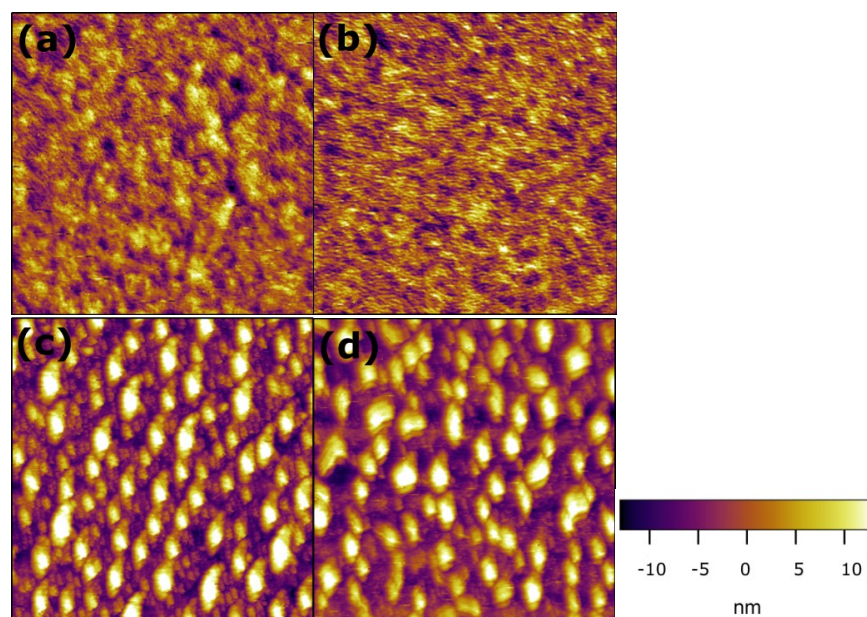


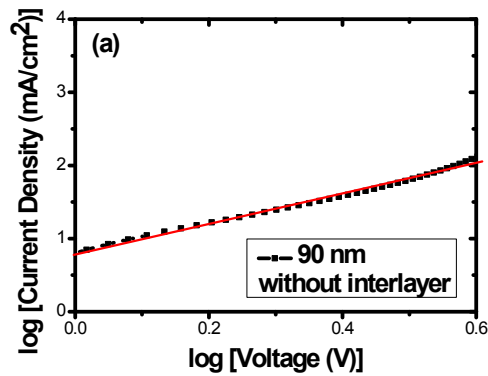
Figure S6 AFM ($5 \times 5 \mu\text{m}$, scan rate is 0.86 Hz) images of blend films without interlayer (a), with PFN (b), with POSS-FN (c), with PStN (d).

4. Field- independence space-charge-limited current mobility measurements.^[S3]

The hole and electron mobilities were calculated by fitting to the Mott-Gurney law, which is expressed by

$$J = 9\epsilon_r\epsilon_0\mu V^2/8L^3 \quad (1)$$

where $\epsilon_r\epsilon_0$ is the dielectric permittivity of the active layer, L is the thickness of the active layer, and μ is the mobility. Under the space charge limited current, we fitted the experimental J - V data with the equation to get the slope of 2 in the logarithmical scales and the mobilities were obtained as field independent values.^[S3]



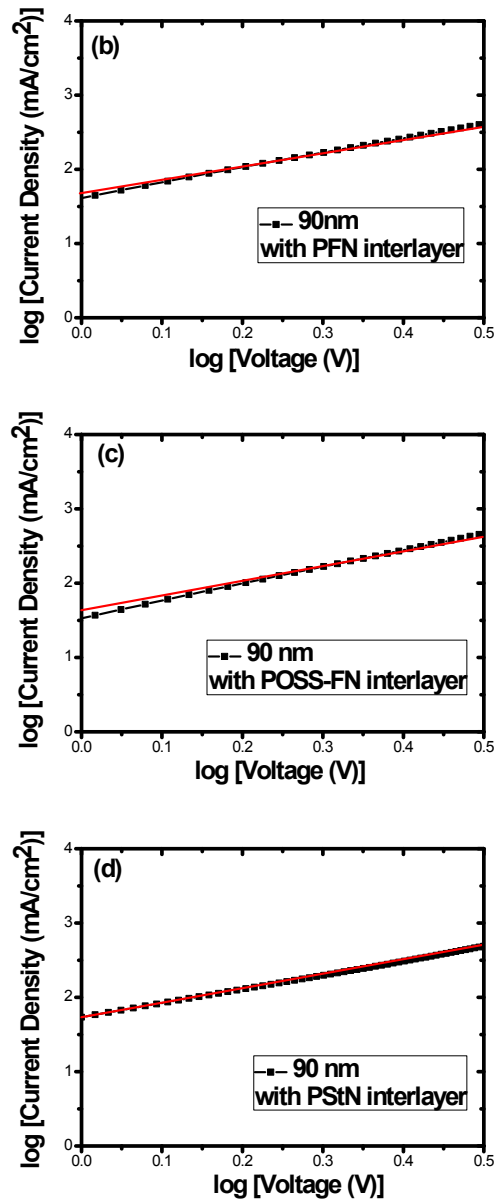


Figure S7 Current density versus applied voltage (J-V) characteristics and corresponding fitting results from SCLC model (black line measured and red line fitted) of hole-only devices ITO substrate/PEDOT:PSS (38 nm)/PBDT-BT:PC₆₁BM (90 nm)/with or without interlayer/MoO_x(8 nm)/Au (40 nm): without interlayer (a), with PFN interlayer (b), with POSS-FN interlayer (c) and with PStN interlayer (d).

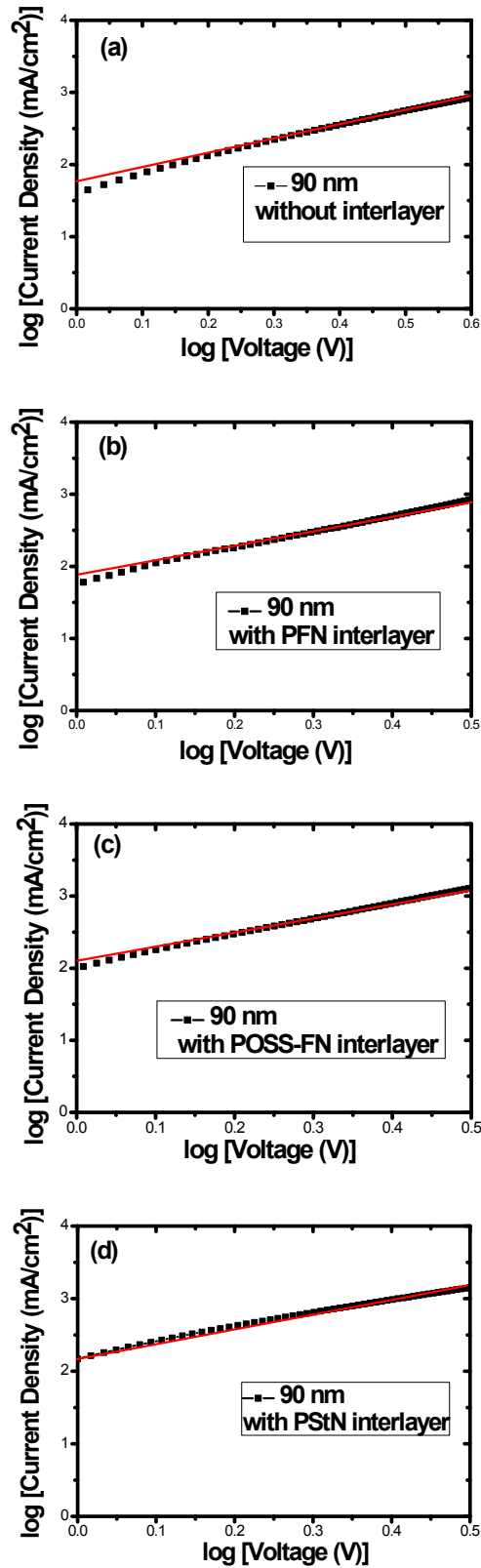


Figure S8 Current density versus applied voltage (J-V) characteristics and corresponding fitting results from SCLC model (black line measured and red line

fitted) of electron-only devices ITO substrate/TIPD (12 nm)/ PBDT-BT:PC₆₁BM (90 nm)/with or without interlayer /Al (100 nm): without interlayer (a), with PFN interlayer (b), with POSS-FN interlayer (c) and with PStN interlayer (d).

5. Surface Energy Measurements

The contact angles were measured through the sessile drop goniometry method (water, methanol, and interlayer solutions) with a CAM 200 (KSV Instrument LID), and the photos were taken with a BASLER A602f-2 camera. The images of the drops and the contact angles are shown in Figure S9 and Table S4.

To compare the effects of surface energy by dynamic of liquids at the various interlayer modified surfaces, we chose three kinds of different polarity liquids, including deionized water, ethylene glycol and *n*-hexadecane, whose surface energies components listed in **Table S4** [S4-S6]. The surface energy of a solid (γ_s) is related to the contact angle of a droplet of the three different known liquids on the surface of the solid, through Young-Dupre equation 2 and 3:

$$\gamma_l(\cos\theta + 1) = 2[(\gamma_s^{LW}\gamma_l^{LW})^{\frac{1}{2}} + (\gamma_s^+\gamma_l^-)^{\frac{1}{2}} + (\gamma_s^-\gamma_l^+)^{\frac{1}{2}}] \quad (2)$$

$$\gamma_s = \gamma_s^{LW} + \gamma_s^{AB} = \gamma_s^{LW} + (\gamma_s^+\gamma_s^-)^{\frac{1}{2}} \quad (3)$$

where γ_s and γ_l are the solid and liquid tension, “s” and “l” means the solid and liquid state, and the dispersive component γ^+ , γ^- are respectively the electron acceptor and donor, contributions to the surface energy of liquid and solid. γ_s^{LW} is the apolar, named the Lifshitz van der Waals interactions, and γ_s^{AB} is the polar acid-base interactions. After measuring the contact angel of the three different liquids, the unknown surface energy contributions of the solid contained in equation 2 can be solved simultaneously.

Interfacial energies of various interlayer modifications were calculated using the well-accepted Good-Girifalco-Fowkerson rule ^[S7] equation 4:

$$\gamma_{ai} = (\sqrt{\gamma_i^{AB}} - \sqrt{\gamma_i^{LW}})^2 + 2(\sqrt{\gamma_a^+ \gamma_i^-} + \sqrt{\gamma_i^+ \gamma_a^-} - \sqrt{\gamma_a^+ \gamma_i^-} - \sqrt{\gamma_a^- \gamma_i^+}) \quad (4)$$

Where “a” and “i” means the active layer and interlayer state, respectively. γ^+ , γ^- are respectively the electron acceptor and donor as well. The situ contact angel experiment data lists in **Table 4**, we calculated the surface and interfacial free energies of various interlayer modification from it, and all of the data are presented in **Table 4** as well.

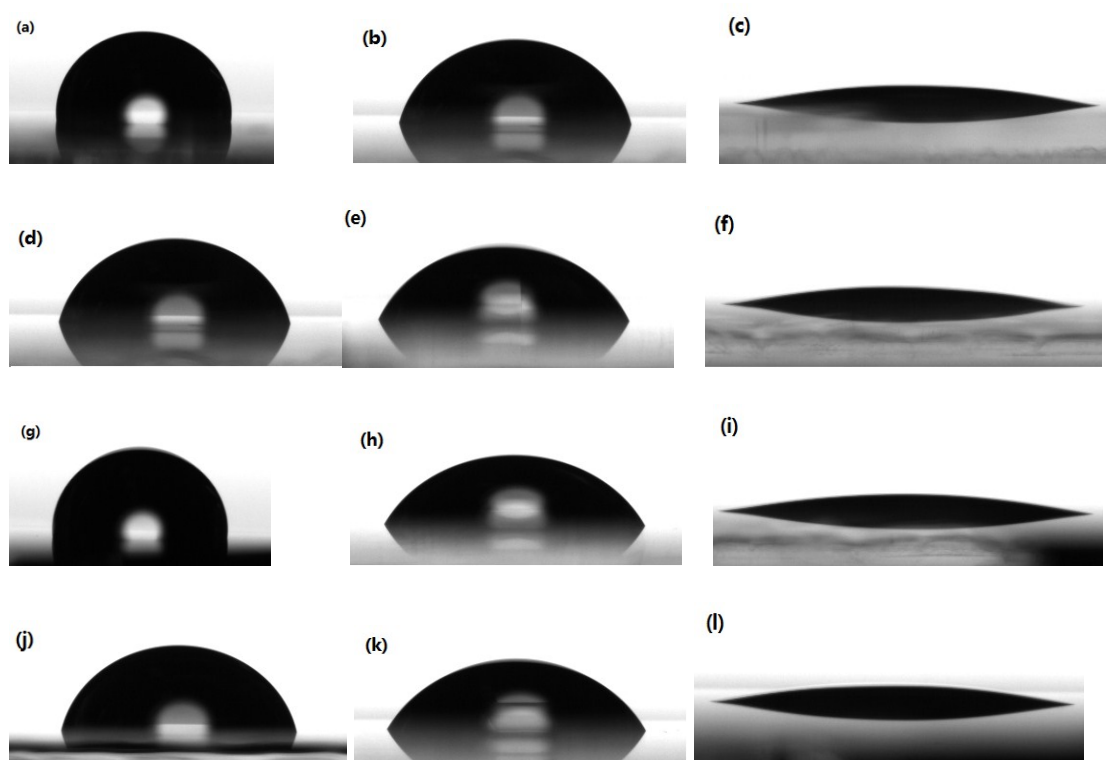


Figure S9 Contact angle images of drops of water (a), ethylene glycol (b) and hexadecane (c) on PBDT-BT: PC₆₁BM films; Contact angle images of drops of water (d), ethylene glycol (e) and hexadecane (f) on PBDT-BT: PC₆₁BM / PFN films; Contact angle images of drops of water (g), ethylene glycol (h) and hexadecane (i) on PBDT-BT: PC₆₁BM / POSS-FN films; Contact angle images of drops of water (j), ethylene glycol (k) and hexadecane (l) on PBDT-BT: PC₆₁BM / PStN films;

Table S4 Surface Energy Components of Three Different Probing Liquids, Used for the Surface Energy Determination. (mN/m)

	γ	γ^{LW}	γ^{AB}	γ^+	γ^-
Water	72.80	21.80	51.00	25.50	25.50
Ethylene Glycol	48.00	29.00	19.00	1.92	47.00
Hexadecane	21.47	27.47	0	0	0

Notes and Reference:

[S1] F. Huang, H. B. Wu, D. G. Wang, W. Yang, Y. Cao, Novel Electroluminescent Conjugated Polyelectrolytes Based on Polyfluorene, *Chem. Mater.* 2004, **16**, 708-716.

[S2] K. Y. Pu, K. Li, B. Liu, Cationic Oligofluorene Substituted POSS as Light-Harvesting Unimolecular Nanoparticle for Fluorescence Amplification in Cellular Imaging, *Adv. Mater.*, 2010, **22**, 643-646.

[S3] P. W. M. Blom, M. C. J. M. Vissenberg, Charge Transport in Poly(p-phenylene vinylene) Light-emitting Diodes, *Mater. Sci. Eng.*, 2000, **27**, 53.

[S4] X. J. Wang, T. Ederth, O. Inganäs, In Situ Wilhelmy Balance Surface Energy Determination of Poly(3-hexylthiophene) and Poly(3,4-ethylenedioxythiophene) during Electrochemical Doping–Dedoping, *Langmuir*, 2006, **22**, 9287-9294.

[S5] M. D. Clark, M. L. Jespersen, R. J. Patel, B. J. Leever, Predicting Vertical Phase Segregation in Polymer-Fullerene Bulk Heterojunction Solar Cells by Free Energy Analysis. *ACS Appl. Mater. Interfaces*, 2013, **5**, 4799-4807.

[S6] L. M. Lander, L. M. Siewieerski, W. J. Brittain, E. A. Vogler, A Systematic Comparison of Contact Angle Methods, *Langmuir*, 1993, **9**, 2237-2239.

[S7] H. K. Nguyen, M. Labardi, S. Capaccioli, M. Lucchesi, P. Rolla, D. Prevosto, Interfacial and Annealing Effects on Primary α -Relaxation of Ultrathin Polymer Films Investigated at Nanoscale, *Macromolecules*, 2012, **45**,2138-2144.